Journal of Alloys and Compounds 519 (2012) 101–105

Contents lists available at SciVerse ScienceDirect

Journal of Alloys and Compounds

journal homepage: www.elsevier.com/locate/jallcom

Magnetism-induced ductility in NiAl intermetallic alloys with Fe additions: Theory and experiment

J. Huang, J. Sun*, H. Xing, Y.F. Wen

School of Materials Science and Engineering, Shanghai Jiaotong University, Shanghai 200240, PR China

ARTICLE INFO

Article history:
Received 10 October 2011
Received in revised form
20 December 2011
Accepted 21 December 2011
Available online 29 December 2011

Keywords:
Intermetallics
Dislocations
Mechanical properties
Computer simulations
Transmission electron microscopy

ABSTRACT

The magnetism-induced ductility in Ni-rich NiAl intermetallic alloys with Fe additions has been investigated theoretically and experimentally. The compressive tests showed that Fe addition decreases the yield strength, but increases the ductility and fracture strength of Ni(Al,Fe) alloys markedly. TEM observations revealed that ⟨0 0 1⟩{1 1 0} is the active slip in Ni(Al,Fe). Theoretical calculations further exhibited that Fe addition mildly reduces the ⟨0 0 1⟩{1 1 0} γ_{GSF} of magnetic Ni(Al,Fe) in comparison to Ni-rich NiAl alloys. The estimated critical stress for moving ⟨0 0 1⟩ dislocations decreases obviously with increasing Fe additions for magnetic Ni(Al,Fe) alloys. These can be considered as the reasons to interpret the magnetism-induced ductility in Ni(Al,Fe) alloys.

1. Introduction

The NiAl intermetallic compound with B2 structure is of great interest for applications in aerospace industry due to its high strength, low density and good oxidation resistance at high temperatures [1,2]. The plastic deformation in NiAl intermetallic compound occurs principally by the motion of ⟨0 0 1⟩ {0 1 1} dislocations in polycrystals and single crystals loaded along non-⟨1 0 0⟩ axe [3]. Therefore, polycrystalline NiAl is brittle at lower temperatures because it lacks sufficient slip systems and cannot meet the requirement of Von Mises principles. The lack of ductility at lower temperatures limits the practical use of NiAl alloys. Many attempts of alloying have been performed to improve the mechanical properties of NiAl alloys [4–10]. For example, Darolia et al. revealed that the ternary addition of Fe significantly improves the tensile ductility of NiAl single crystals loaded at the non-⟨0 0 1⟩ directions [4]. Recently, Liu et al. and Fu et al. observed the solid solution softening effects of ternary additions of Fe and Mn in Ni-rich Ni-40% Al alloys by hardness measurements [11,12]. The theoretical calculations and experimental measurements indicated that the site preferences of Fe and Mn solute atoms on the Al sublattices are magnetically driven. The unusual solid solution softening were interpreted from lattice expansion induced by the magnetic coupling between solute and host atoms and reduction of the shear modulus of the alloys, and therefore, called the magnetism-induced solid solution softening [11,12].

Basically, the brittle/ductile behavior of a solid material can be described by two competing issues at atomistic scale: *i.e.* the cleavage and emission of dislocations at the crack tip [13,14]. The emission of dislocations at the crack tip blunts the crack and leads to ductile behavior, which is characterized theoretically by the unstable stacking fault energy γ_{us}. The γ_{us} is defined as the maximum of the generalized stacking fault energy γ_{GSF}, which is associated with the shear displacement of the crystal along the slip plane [14,15]. Moreover, the γ_{us} is related to the Peierls stress of dislocations and governs the mobility of dislocations. Thus, it is critical to deeply understand the influence of alloying elements on the unstable stacking fault energy of the B2 NiAl alloys. Hong and Freeman calculated the anti-phase boundary (APB) energies, the local minimum energies from the ⟨1 1 1⟩{1 1 0} γ_{GSF} profiles at displacement of $a/2$ ⟨1 1 1⟩ in pure NiAl and its alloys with ternary additions of V, Cr and Mn [16]. They found that the APB energy of pure NiAl is extremely high and the ternary additions significantly reduce the APB energies of the NiAl alloys. Lazar et al. also investigated the influence of ternary additions, such as Cr, Mo, Ti and Ga on the unstable stacking fault energy and cleavage energy of NiAl by *ab initio* approach [17]. Based on the calculated results, they estimated a possible ductility improvement of the ternary NiAl alloys according to the Rice's criterion. Very recently, Lazar et al. calculated the generalized stacking fault energies and magnetisms of NiAl alloys with additions of Fe and Mn [18]. All those calculations were performed for the pure NiAl and its alloys with ternary additions. For

* Corresponding author. Tel.: +86 21 54745593; fax: +86 21 54745593.
E-mail address: jsun@sjtu.edu.cn (J. Sun).

0925-8388/$ – see front matter © 2012 Elsevier B.V. All rights reserved.
doi:10.1016/j.jallcom.2011.12.101

the solid solution softening effects were observed in Ni-rich NiAl alloys with ternary additions, it is necessary to calculate the generalized stacking fault energy of Ni-rich NiAl alloy to understand comprehensively the mechanism of magnetism-induced ductility in NiAl alloys with Fe additions.

In this paper, the magnetism-induced ductility in Ni-rich NiAl intermetallic alloys with Fe additions has been verified by compressive tests. The deformed microstructures of the alloys were observed by electron transmission microscopy (TEM) to reveal the active slip of dislocations. As expected theoretically, application of the generalized stacking model should be able to probe the physical nature of the effect of Fe additions on the mechanical properties of the NiAl alloys. The generalized stacking fault energies along $\langle 1\,0\,0\rangle\{0\,1\,1\}$ and $\langle 1\,1\,1\rangle\{0\,1\,1\}$ and elastic properties, such as elastic constants and moduli of Ni-rich and Ni(Al,Fe) alloys were calculated by *ab initio* approach. The effect of magnetism on the generalized stacking fault energy of Ni(Al,Fe) was also calculated in this paper. Based on these calculated results, the mechanism of magnetism-induced ductility in NiAl intermetallic alloys with Fe additions is finally discussed.

2. Experimental and computational details

The NiAl intermetallic alloys with different contents of Fe additions were prepared by arc-melting in vacuum. The nominal chemical compositions (at.%) of the alloys are $Ni_{60}Al_{40}$, $Ni_{54}Al_{40}Fe_6$, $Ni_{52}Al_{40}Fe_8$, $Ni_{50}Al_{40}Fe_{10}$, respectively. The ingots underwent homogenizing heat treatment at 1100 °C for 96 h and then cooled down in the furnace. The specimens with a size of 4 mm × 4 mm × 8 mm were wire-cut from the ingots for compressive tests. The compressive tests were conducted on Shimadzu mechanical machine at room temperature and at strain rate of $10^{-4}\,s^{-1}$. TEM samples were prepared by twin jet electro-polishing in a perchloric acid and ethanol solution chilled to −30 °C at 30 V. The microstructures of the deformed alloys were observed by JEM-2100F microscope operating at 200 kV.

Ab initio calculations based on the density functional theory (DFT) implemented in the *Vienna ab initio* Simulation Package (VASP) were performed in this work [19]. The projector augmented wave (PAW) method was used for the construction of potentials [20]. Perdew-Wang generalized gradient approximation (GGA) was adopted to treat the exchange-correlation density function [21]. The convergence accuracy of total energy calculations was chosen as 10^{-6} eV and the plane-wave energy cutoff 400 eV. Atomic relaxations were allowed whenever the structural relaxations were required.

To calculate the elastic properties, a 16-atom supercell for Ni-rich NiAl and Ni(Al,Fe) alloys was employed, in which the extra Ni or Fe atoms occupy the Al sublattice. The nominal chemical composition of Ni-rich NiAl and Ni(Al,Fe) is $Ni_{62.5}Al_{37.5}$, $Ni_{56.25}Al_{37.5}Fe_{6.25}$ and $Ni_{50}Al_{37.5}Fe_{12.5}$, respectively. A 9 × 9 × 9 k-mesh was used for k points sampling for the supercell according to the Monkhorst–Pack scheme [22]. The elastic constants were evaluated by means of the total energies calculated as a function of applied strains using the volume conserving tetragonal or monoclinic deformation [23]. The elastic moduli were estimated by the method described elsewhere [24,25].

To calculate the generalized stacking fault (GSF) energy, a 48-atom supercell of $e_1 \times e_2 \times 9e_3$ with $e_1 = [0\,0\,\bar{2}]$, $e_2 = [1\,1\,\bar{1}]$ and $e_3 = [1\,\bar{1}\,0]$, respectively was used to establish a slab with thickness of $6e_3$ (12-atomic layers) and vacuum of $3e_3$ along the $\langle 1\,\bar{1}\,0\rangle$ direction. A 7 × 7 × 1 k-mesh was used for k points sampling for the supercell. The stacking faults of $\langle 0\,0\,1\rangle\{1\,1\,0\}$ or $\langle 1\,1\,1\rangle\{1\,1\,0\}$ were generated by shifting the upper half of the slab relative to the lower half with different displacement vectors along the $\langle 0\,0\,1\rangle$ or $\langle 1\,1\,1\rangle$ direction on the $(1\,\bar{1}\,0)$ plane, respectively. Atomic relaxation of the supercell was done in the direction vertical to the slip plane. The generalized stacking fault energies were obtained from the energy difference per unit area between the supercells with and without displacement. For Ni-rich NiAl, one Ni atom substitutes for Al, causing 25 at.% extra Ni in the slip plane and 2.1 at.% in the supercell, respectively. Similarly, one Fe atom substitutes for Al, causing 25 at.% Fe in the slip plane and 2.1 at.% in the supercell, respectively for Ni(Al,Fe). It is noteworthy that the spin polarization was activated in the calculations of Ni(Al,Fe) to elucidate the role of magnetism in the mechanical properties of the alloys.

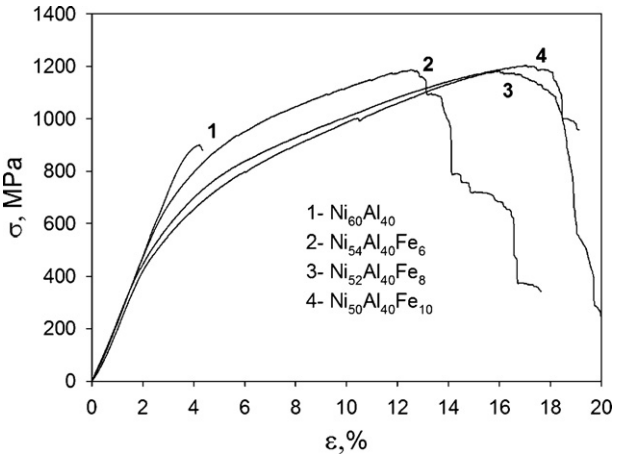

Fig. 1. Compressive stress–strain curves of Ni-rich NiAl and Ni(Al,Fe) intermetallic alloys.

3. Results and discussion

3.1. Compressive deformation and substructure

Fig. 1 shows the compressive stress–strain curves of the Ni-rich NiAl and Ni(Al,Fe) intermetallic alloys. The yield strength deceases obviously from 873 MPa in $Ni_{60}Al_{40}$ to 473 MPa in $Ni_{50}Al_{40}Fe_{10}$. The compressive ductility increases markedly from 0.75% in $Ni_{60}Al_{40}$ to 19.5% in $Ni_{50}Al_{40}Fe_{10}$, and the fracture strength also increases from 900 MPa in $Ni_{60}Al_{40}$ to 1180 MPa in $Ni_{50}Al_{40}Fe_{10}$. The compressive tests clearly showed that the solid solution softening and ductility enhancement occur in the Ni-rich NiAl alloys with Fe additions, which is in agreement with the results achieved by Darolia et al. and Liu et al., respectively [4,11,12]. A typical dislocation structure of the deformed Ni(Al,Fe) alloys is shown in Fig. 2. Dislocations are relatively uniformly distributed in the microstructure and evidence of slip band does not appear. These structures with zig-zag shaped and bowed segments are produced by the kinking phenomenon. The diffraction contrast analyses performed with different reflections revealed that $\langle 0\,0\,1\rangle\{1\,1\,0\}$ is the active slip system in Ni(Al,Fe) alloys. Darolia et al. had already revealed that the ternary addition of Fe improves significantly the tensile ductility of NiAl single crystals loaded at the $\langle 1\,1\,0\rangle$ and $\langle 1\,1\,1\rangle$ directions, rather than the $\langle 0\,0\,1\rangle$ direction [4]. This also implies that $\langle 0\,0\,1\rangle\{1\,1\,0\}$ is the active slip and Fe addition cannot activate the $\langle 1\,1\,1\rangle$ slip system in Ni(Al,Fe) single crystals.

3.2. Theoretical elastic modulus

Table 1 shows the calculated lattice parameters, magnetic moments and elastic constants of the Ni-rich NiAl and Ni(Al,Fe) alloys. The theoretical lattice parameter of $Ni_{62.5}Al_{37.5}$ is larger compared with the experimental one, but the elastic constants of $Ni_{62.5}Al_{37.5}$ are well consistent with the experimental results

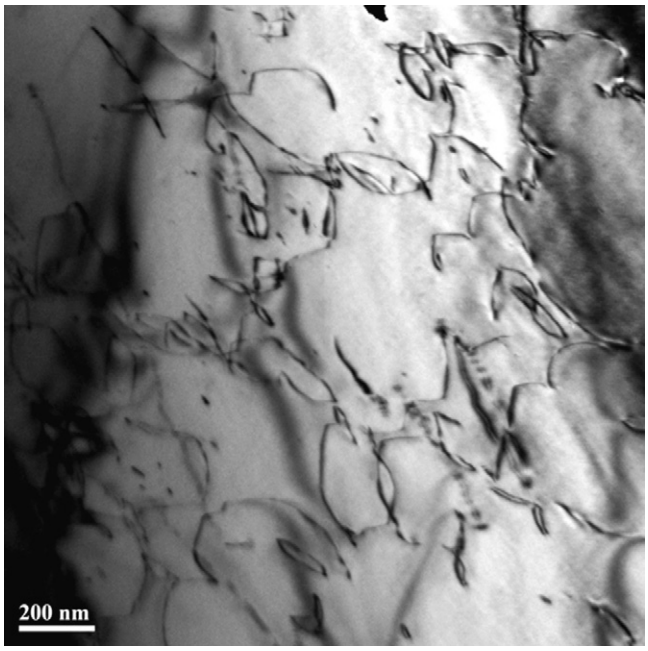

Fig. 2. Dislocation structure of the deformed Ni(Al,Fe) alloys.

Table 1
Lattice parameter (Å), magnetic moment (μ_B) and elastic constant (GPa) of Ni-rich NiAl and magnetic Ni(Al,Fe) alloys.

	a_0	M	C_{11}	C_{12}	C_{44}
$Ni_{62.5}Al_{37.5}$	2.860 2.836 [26]	0	170.7 169.7 [26]	161.0 159.3 [20]	127.7 120.0 [26]
$Ni_{56.25}Al_{37.5}Fe_{6.25}$ (mag.)	2.869	3.149	172.1	147.6	120.4
$Ni_{50}Al_{37.5}Fe_{12.5}$ (mag.)	2.877	5.881	180.7	144.3	109.1

Table 2
Elastic moduli (GPa) of Ni-rich NiAl and magnetic Ni(Al,Fe) alloys.

	$(C_{11}-C_{12})/2$	E	G_V	G_R	G_H	G_H/B	ν
$Ni_{62.5}Al_{37.5}$	4.9 6.0 [12]	123.7	78.6 84 [12]	11.5	45.0	0.274	0.374
$Ni_{56.25}Al_{37.5}Fe_{6.25}$ (mag.)	12.3 13.5 [12]	140.0	77.1 80 [12]	26.6	51.9	0.333	0.350
$Ni_{50}Al_{37.5}Fe_{12.5}$ (mag.)	18.2 19.0 [12]	146.7	72.7 77 [12]	36.4	54.6	0.349	0.344

[26]. The calculated lattice parameters increase with increasing Fe additions in the alloys, which is again in agreement with the experimental observations [11,12]. Unlike Ni-rich NiAl, Ni(Al,Fe) alloys show large magnetic moments, and the magnetic moments increase with increasing Fe additions in the alloys. The reason that the substitution of Fe for Al leads to an increase of the lattice parameter has been considered to arise from the magnetic coupling between solute and host atoms in Ni(Al,Fe) alloys [11,12,27]. Therefore, the ductility enhancement occurring in the Ni-rich NiAl alloys with Fe additions can be considered to be related to the magnetism of the alloys.

The calculated moduli of the Ni-rich NiAl and magnetic Ni(Al,Fe) alloys are presented in Table 2. Generally, Voigt, Reuss and Hill approximations can be used to estimate the shear modulus from the elastic constants of the alloys [24,25]. Among them, the Hill approximation is employed most widely and reasonably to calculate the shear modulus in polycrystalline materials for it is the arithmetic average of Voigt and Reuss approximations, corresponding to the upper and lower limits of the shear modulus, respectively. In the present calculations, the Hill approximation used to estimate

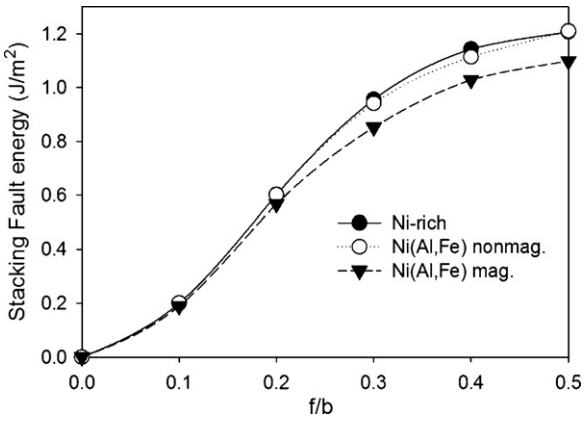

Fig. 3. Generalized stacking fault energies of {1 1 0} ⟨0 0 1⟩ for Ni-rich NiAl and Ni(Al,Fe) alloys, where f is the shear displacement along slip plane and b is a ⟨0 0 1⟩.

the shear modulus of the alloys. Table 2 shows that in $Ni_{62.5}Al_{37.5}$, the substitution of Ni for Al significantly reduces the tetragonal shear modulus $(C_{11}-C_{12})/2$, Young's modulus E and shear modulus G compared with those in the stoichiometric NiAl [28,29], which suggests the cubic materials trend to be mechanically unstable due to the shape memory effect. In comparison to $Ni_{62.5}Al_{37.5}$, the tetragonal shear modulus, Young's modulus increase with increasing Fe additions for magnetic Ni(Al,Fe) alloys. The shear modulus calculated by Hill approximation shows the same trend as the tetragonal shear modulus and Young's modulus, but that calculated by Voigt approximation decreases with increasing Fe additions for magnetic Ni(Al,Fe) alloys, as shown in Table 2. Fu et al. calculated the elastic constants and estimated the shear modulus by Voigt approximation, and they also found that the shear modulus decreases linearly with increasing Fe additions for Ni(Al,Fe) alloys (see Table 2), which was considered as one of the reasons to explain the solid solution softening effects in Ni(Al,Fe) alloys [12]. However, the present calculated results showed that the tetragonal shear modulus, Young's modulus and shear modulus estimated by Hill approximation increase with increasing Fe additions, which could not interpret the magnetism-induced softening in magnetic Ni(Al,Fe) alloys.

On the other hand, the ductile/brittle behavior of materials is empirically related to the ratio G/B or Poisson's ratio ν according to Pugh [30]. The lower the value of G/B or the higher the value of ν, the more ductile the materials would be. Based on the ratio G/B and Poison's ratio ν, the Ni-rich NiAl is more ductile than Ni(Al,Fe) alloys. This is again in disagreement with the experimental results described above. The magnetism-induced ductility occurring in magnetic Ni(Al,Fe) alloys could be hardly related to the difference of the elastic properties between Ni-rich NiAl alloys with and without Fe additions.

3.3. Theoretical slip property

In B2 NiAl, there are two possible operative slips in the {1 1 0} plane. ⟨0 0 1⟩{1 1 0} is the perfect dislocation, whereas ⟨1 1 1⟩{1 1 0} dissociates into a pair of superpartial dislocations bounding an antiphase boundary (APB). The calculated GSF energies γ_{GSF} of the ⟨0 0 1⟩{1 1 0} and ⟨1 1 1⟩{1 1 0} slip systems of the Ni-rich NiAl and Ni(Al,Fe) alloys are shown in Figs. 3 and 4, respectively. The APB energies γ_{APB}, the local minimum energies can be achieved from the ⟨1 1 1⟩{1 1 0} γ_{GSF} profiles at $f/b = 0.5$. The unstable stacking fault energies γ_{us}, the maximum energies from the ⟨1 1 1⟩{1 1 0} γ_{GSF} profiles are located at $f/b = \sim 0.3$, which are not dictated by symmetry. The unstable stacking fault energies for each slip system and the APB energies are summarized in Table 3. In Ni-rich NiAl, the

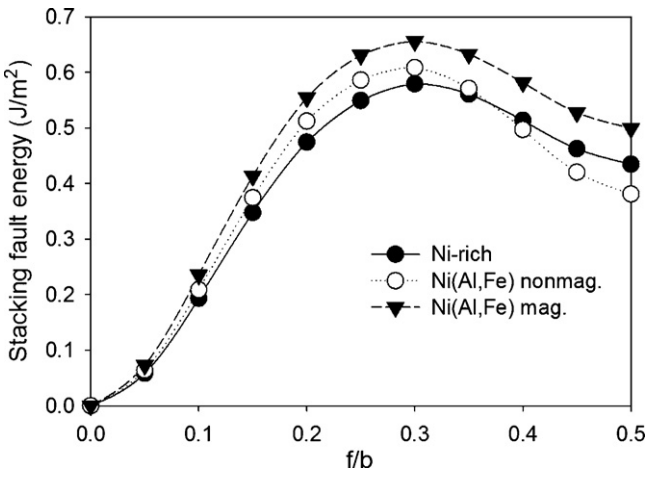

Fig. 4. Generalized stacking fault energies of {1 1 0}⟨1 1 1⟩ for Ni-rich NiAl and Ni(Al,Fe) alloys, where *f* is the shear displacement along slip plane and *b* is *a*/2 ⟨1 1 1⟩.

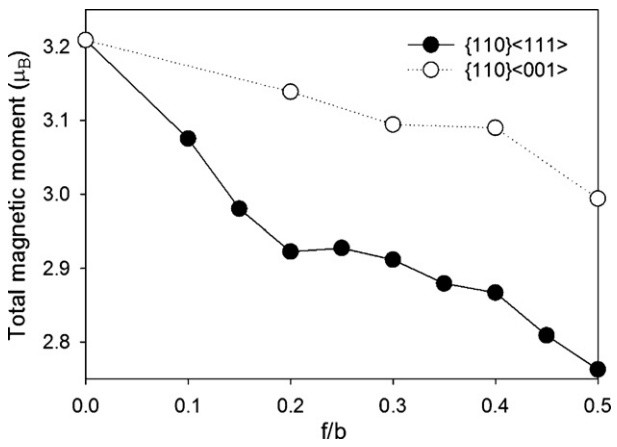

Fig. 5. Total magnetic moment for the ⟨0 0 1⟩{1 1 0} and ⟨1 1 1⟩{1 1 0} slip path for magnetic Ni(Al,Fe) alloy.

Table 3
Calculated unstable stacking fault energy (J/m²) and APB energy (J/m²) for ⟨0 0 1⟩{1 1 0} and ⟨1 1 1⟩{1 1 0} of Ni-rich NiAl and Ni (Al,Fe).

	γ_{us} ⟨0 0 1⟩	γ_{us} ⟨1 1 1⟩	γ_{APB}
Ni-rich NiAl	1.21	0.55	0.44
Ni(Al,Fe) (mag.)	1.10	0.66	0.50
	1.16 [18]	0.64 [18]	0.45 [18]
Ni(Al,Fe) (non-mag.)	1.21	0.59	0.38

⟨0 0 1⟩{1 1 0} γ_{us} is much higher than ⟨1 1 1⟩{1 1 0}, which implies more difficult for the nucleation of ⟨0 0 1⟩{1 1 0} than ⟨1 1 1⟩{1 1 0}. However, the experimental results had already indicated that the dominant slip system is ⟨0 0 1⟩{1 1 0} rather than ⟨1 1 1⟩{1 1 0} in Ni-rich NiAl [31]. It has been suggested that the active ⟨0 0 1⟩{1 1 0} slip in NiAl is a consequence of the relatively high APB energy and weak repulsive elastic force between partial dislocation that make dissociation of ⟨1 1 1⟩ superdislocations into partial dislocations unlikely [32]. Although the APB energy of 0.44 J/m² in Ni-rich NiAl is much lower than that of 0.76 J/m² in the stoichiometric NiAl [17], the reduction of APB energy is probably not large enough to activate the ⟨1 1 1⟩{1 1 0} slip in Ni-rich NiAl alloys.

Table 3 shows that the substitution of Fe for Al decreases slightly the ⟨0 0 1⟩{1 1 0} γ_{GSF} of the magnetic Ni(Al,Fe) in comparison to Ni-rich NiAl. And the ⟨1 1 1⟩{1 1 0} γ_{GSF} of the magnetic Ni(Al,Fe) is mildly higher than that of Ni-rich NiAl. The present results are comparable to those calculated by Lazar et al. [18]. It is noted that a 24-atom supercell was used in their calculation and the content of Fe additions in the slip plane is 50 at.% for Ni(Al,Fe) [18], which is different from the computational conditions described above in this work. The ⟨0 0 1⟩{1 1 0} and ⟨1 1 1⟩{1 1 0} γ_{GSF} of the non-magnetic Ni(Al,Fe) are close to those of Ni-rich NiAl, rather than those of the magnetic Ni(Al,Fe), which implies that magnetism plays an important role on the planar defect property in Ni(Al,Fe) alloys. Fig. 5 shows variations of the total magnetic moments as a function of the slip displacement in both ⟨0 0 1⟩{1 1 0} and ⟨1 1 1⟩{1 1 0} slip systems in the magnetic Ni(Al,Fe) alloys. The total magnetic moments simultaneously decrease with the slip displacement along the ⟨0 0 1⟩{1 1 0} and ⟨1 1 1⟩{1 1 0} slip path. The initial magnetic moment of 3.21 μ_B is reduced by 0.22 μ_B at the 1/2 ⟨0 0 1⟩ slip displacement, whereas by 0.45 μ_B at the 1/2 ⟨1 1 1⟩ slip displacement in Ni(Al,Fe). These variations derive from a change of local circumstance of the Fe atom in Ni(Al,Fe).

The theoretical results indicated that the ⟨0 0 1⟩{1 1 0} γ_{us} is much higher than ⟨1 1 1⟩{1 1 0} in magnetic Ni(Al,Fe) alloys, which is the same as that in Ni-rich NiAl. However, the experimental results mentioned above and those obtained by Darolia et al. [4] confirmed that ⟨0 0 1⟩{1 1 0} is still the active slip system in the ductilized Ni(Al,Fe) alloys. It was reported that in B2 FeAl, the active slip system is ⟨1 1 1⟩{1 1 0} rather than ⟨0 0 1⟩{1 1 0} and the APB energy of the {1 1 0} plane had been determined to be 0.11 J/m² [33]. If one takes the APB energy of FeAl as a reference for APB to occur, the APB energy of Ni(Al,Fe) alloys is still probably too high to activate the ⟨1 1 1⟩{1 1 0} slip. As the γ_{us} is related to the Peierls stress of dislocations and governs the mobility of dislocations, only small reduction of the ⟨0 0 1⟩{1 1 0} γ_{us} of the magnetic Ni(Al,Fe) compared with Ni-rich NiAl can be related to the magnetism-induced ductility in Ni(Al,Fe) from the viewpoint of γ_{GSF}. Moreover, early atomistic simulations performed by Yamaguchi et al. indicated that the core structure of the ⟨0 0 1⟩ screw dislocations in B2 NiAl spreads into the {1 1 0} plane and the critical stress for the dislocation movement is 7×10^{-3} C_{44} [34]. Using the elastic constants listed in Table 1, the critical stress for moving ⟨0 0 1⟩ dislocations can be evaluated to be 894 MPa for $Ni_{62.5}Al_{37.5}$, 843 MPa for $Ni_{50}Al_{37.5}Fe_{6.25}$ and 764 MPa for $Ni_{50}Al_{37.5}Fe_{12.5}$ alloys, respectively. This is consistent with the decreasing trend of the yield strength with increasing Fe additions in magnetic Ni(Al,Fe) alloys as shown in Fig. 1, although the estimated critical stresses are much higher than the compressive yield strengths in Ni(Al,Fe) alloys. Therefore, the mechanism of the magnetism-induced ductility in Ni(Al,Fe) alloys can be attributed to the decrease of the critical stress for moving ⟨0 0 1⟩ dislocations with increasing Fe additions in magnetic Ni(Al,Fe) alloys. It is worthwhile to mention that in addition to the line and planar defect properties discussed above, the properties of the point defects, such as antisite defects and vacancies and the interactions between point defects and dislocations certainly affect the mechanical properties of the strongly ordered NiAl alloys. The influence of the ternary addition on the point defect properties in NiAl alloys needs to be further investigated and correlated with the mechanical properties of the ternary NiAl alloys.

4. Conclusions

The compressive tests showed that Fe addition markedly decreases the yield strength but increases the ductility and fracture strength of Ni(Al,Fe) compared with Ni-rich NiAl alloys. TEM observations revealed that ⟨0 0 1⟩{1 1 0} is the active slip system in Ni(Al,Fe). Theoretical calculations further exhibited that the lattice parameter, associated with large magnetic moment increases with increasing Fe additions for Ni(Al,Fe). The elastic moduli of magnetic Ni(Al,Fe) are higher than those of Ni-rich NiAl alloys. For the slip properties, Fe addition mildly reduces the ⟨0 0 1⟩{1 1 0} γ_{GSF} of

magnetic Ni(Al,Fe) in comparison to Ni-rich NiAl alloys. Furthermore, the estimated critical stress for moving ⟨0 0 1⟩{1 1 0} dislocations obviously decreases with increasing Fe additions for the magnetic Ni(Al,Fe) alloys. It can be concluded that addition of magnetic Fe elements significantly enhances the ductility of Ni-rich NiAl alloys, the mechanism of which can be attributed to the decrease of the critical stress for moving ⟨0 0 1⟩{1 1 0} dislocations in magnetic Ni(Al,Fe) alloys.

Acknowledgements

The authors would like to acknowledge the financial support from the National Natural Science Foundation of China (Grant No. 50871065) and the Science and Technology Committee of Shanghai Municipal (Grant No. 09JC1407200 & 10DZ2290904).

References

[1] R.D. Noebe, R.R. Bowman, M.V. Nathal, Int. Mater. Rev. 38 (1993) 193–232.
[2] D.B. Miracle, R. Darolia, in: J.H. Westbrook, R.L. Fleischer (Eds.), Structural Applications of Intermetallic Compounds, Wiley, London, 2000, pp. 55–74.
[3] J.T. Kim, Ph D. Thesis, University of Michigan, Ann Arbor, MI, 1990.
[4] R. Darolia, D. Larman, R.D. Field, Scripta Metall. Mater. 26 (1992) 1007–1012.
[5] G.P. Cammarota, A. Casagrande, J. Alloys Compd. 381 (2004) 208–214.
[6] L.M. Peng, J. Alloys Compd. 440 (2007) 150–153.
[7] C.Y. Cui, J.T. Guo, H.Q. Ye, J. Alloys Compd. 463 (2008) 263–270.
[8] H.L. Wu, H.B. Guo, S.K. Gong, J. Alloys Compd. 492 (2010) 295–299.
[9] J. Colin, S. Serna, B. Campillo, R.A. Rodriguez, J. Juarez-Islas, J. Alloys Compd. 489 (2010) 26–29.
[10] J.F. Zhang, J. Shen, Z. Shang, Z.R. Feng, L.S. Wang, H.Z. Fu, Intermetallics 21 (2012) 18–25.
[11] C.T. Liu, C.L. Fu, M.F. Chisholm, J.R. Thompson, Maja Krcmar, X.-L. Wang, Prog. Mater. Sci. 52 (2–3) (2007) 352–370.
[12] C.L. Fu, C.T. Liu, X.L. Wang, M. Krcmar, J.A. Fernandez-Baca, Intermetallics 12 (2004) 911–919.
[13] J.R. Rice, R.M. Thomson, Philos. Mag. 29 (1974) 73–97.
[14] J.R. Rice, J. Mech. Phys. Solids 40 (1992) 239–271.
[15] V. Vitek, Philos. Mag. 18 (1968) 773–786.
[16] T. Hong, A.J. Freeman, Phys. Rev. B 43 (1990) 6446–6458.
[17] P. Lazar, R. Podloucky, Phys. Rev. B 73 (2006) 104114.
[18] P. Lazar, R. Podloucky, Intermetallics 17 (2009) 675–679.
[19] G. Kresse, J. Furthmüller, Phys. Rev. B 54 (1996) 11169–11186.
[20] P.E. Blöchl, Phys. Rev. B 50 (1994) 17953–17979.
[21] J.P. Perdew, J.A. Chevary, S.H. Vosko, K.A. Jackson, M.R. Pederson, D.J. Singh, Carlos Fiolhais, Phys. Rev. B 46 (1992) 6671–6687.
[22] H.J. Monkhorst, J.D. Pack, Phys. Rev. B 13 (1976) 5188–5192.
[23] M.J. Mehl, J.E. Osburn, D.A. Papaconstantopoulos, B.M. Klein, Phys. Rev. B 41 (1990) 10311–10323.
[24] R. Hill, Proc. Phys. Soc. 65 (1952) 349.
[25] J. Sun, Q. Yao, H. Xing, W.Y. Guo, J. Phys. Condens. Matter. 19 (2007) 486215.
[26] T. Dacenport, L. Zhou, J. Trivisonno, Phys. Rev. B 59 (1999) 3421–3426.
[27] C.T. Liu, C.L. Fu, L.M. Pike, D.S. Easton, Acta Mater. 50 (2002) 3203–3210.
[28] N. Rusovic, H. Waelimont, Phys. Status. Solidi A 44 (1977) 609–619.
[29] C.A. Moose, M.S. Thesis, Pennsylvania State University, 1991.
[30] S.F. Pugh, Philos. Mag. 45 (1954) 823.
[31] P.R. Munroe, I. Baker, Scripta Metall. 23 (1989) 495–499.
[32] M.H. Yoo, T. Takasugi, S. Hanada, O. Izumi, Mater. Trans. 31 (1990) 435–442.
[33] R.C. Crawford, I.L.F. Ray, Philos. Mag. 35 (1977) 549.
[34] M. Yamaguchi, Y. Umakoshi, Scripta Metall. 9 (1975) 637–640.